

MECHANICAL PROPERTIES AND BIOLOGICAL RESPONSES OF BIOACTIVE GLASS CERAMICS PROCESSED USING INDIRECT SLS

KW Dalgarno¹, DJ Wood², RD Goodridge³, K Xiao¹, C Ohtsuki³, P Genever⁴ & J Dyson¹

¹ School of Mechanical Engineering, University of Leeds, Leeds, LS2 9JT, UK.

² Dental Institute, University of Leeds, Leeds, LS2 9JT, UK.

³ Graduate School of Materials Science, Nara Institute of Science and Technology, 8916-5 Takayama, Ikoma, Nara, 630-0192, Japan.

⁴ Department of Biology (Area 9), PO Box 373, University of York, York, YO10 5YW, UK.

Reviewed, accepted August 25, 2005

Abstract

This paper will report on research which aims to generate bone replacement components by processing bioactive glass-ceramic powders using indirect selective laser sintering. The indirect SLS route has been chosen as it offers the ability to tailor the shape of the implant to the implantation site, and two bioactive glass ceramic materials have been processed through this route: apatite-mullite and apatite-wollastonite. The results of bend tests, to investigate mechanical properties, and *in vitro* and *in vivo* experiments to investigate biological responses of the materials will be reported, and the suitability of completed components for implant will be assessed.

1. Introduction

A wide range of researchers have identified the potential for layer manufacture systems to deliver implants which are personally tailored to the individual patient, and which have been created in materials which will interact positively with the body (rather than be biologically inert). State of the art commercially in this area is Therics™ [1]. Therics™ manufacture, using 3D printing layer manufacture technology, a range of bone grafts and bone void fillers. The layer manufacture technology is not used to create bone void fillers which conform directly to the void shape, but it is used to create complex internal architectures in a small range of products, with structured internal porosity to support bone ingrowth and subsequent vascularisation [2]. The materials used by Therics™ are resorbable (and so over time they will be broken down by the body and replaced with natural bone) and are based on hydroxyapatite and tricalcium-phosphate materials held in a polymer matrix.

The ability to develop their approach to create personalised shapes is something which Therics™ may develop in the future. In the research arena a number of research groups have examined the scope for the creation of bone replacements or tissue engineering scaffolds, with the tissue engineering scaffolds aimed at both hard and soft tissues. The tissue engineering scaffold approach operates through first creating a structure (the scaffold) and then seeding this structure *in vitro* with stem cells and proteins. The stem cells will then proliferate and differentiate into the required type of cell whilst secreting the extracellular matrix required to create the type of tissue needed. Once the type of tissue desired has been created implantation occurs.

Much of the work aimed at producing tissue engineering scaffolds has looked to exploit a range of layer manufacturing techniques to create scaffolds in resorbable polymers, notably poly-

(ϵ -caprolactone) [3,4], poly(L)lactide (PLA) [5], and poly(propylene fumarate) [6]. In addition a number of polymer-ceramic composite materials have been fabricated, using PLA and hydroxyapatite [5], and poly (D,L-lactide-co-glycolide) and tricalcium phosphate [7]. Hydroxyapatite and tricalcium phosphate are both bioceramics, and so by definition have chemical compositions close to the mineral content of bone, and their use together with resorbable polymers seeks to create a more biomimetic material, as bone itself can be considered to be a polymer/ceramic (collagen/calcium phosphate) composite [8]. Collagen itself has also been used with layer manufacture methods to create a tissue engineering scaffold [9]. Collagen is a natural hydrogel (a colloidal gel in which water is the dispersion medium) and this has inspired work with other hydrogel materials [10]. In all of the cases where tissue engineering scaffolds have been created using layer manufacture methods the ability of the layer manufacture techniques to (i) create biomimetic architectures, and (ii) create a scaffold which can be adapted to a required geometry, have been cited as major advantages of the routes.

A number of researchers have also investigated processing bioceramics for bone replacement and tissue engineering applications [11,12], and our work in this area has focussed on processing bioceramics, in particular apatite-mullite (A-M) and apatite-wollastonite (A-W), with bone replacement or hard tissue engineering scaffolds the intended application areas. Initial studies [13] were based on direct SLS, but indirect approaches have proved more capable in terms of delivery of coherent components [14]. This paper outlines recent research outcomes for both A-M and A-W, with reference to both mechanical and biological properties.

2. Processing Routes

The bioceramic powders have been produced within the Leeds Dental Institute, using a melt quenching technique [15,16]. For both A-M and A-W the glass frit using this technique has then been ground to a powder and sieved to give a range of particle sizes. Powder with particles in the range 45-90 μm have been used for SLS, offering the best play-off between ease of spreading in manufacture and the definition of the green parts produced. In some cases a mixture of 45-90 μm size powder and 0-45 μm powder has been used to increase the bed density. Prior to processing the powders have been mixed with 5% by volume of a powder acrylic binder. 5% binder has been found to be the minimum level of binder which results in green parts which are capable of being handled without damage occurring in the green stage. The SLS stage was carried out on an experimental SLS machine at the University of Leeds, which has a 250W CO₂ laser, and is fully described elsewhere [15]. In the laser sintering stages a wide processing window is available with indirect SLS, with laser powers ranging up to 60W, and scan speeds of up to 800mm/s. Table 1 summarises the processing conditions used with each of the two materials to create green parts. SLS was carried out in an air atmosphere.

Once the green parts have been created the next stage in the process is to post-process the components through a heat treatment to burn off the binder, sinter the powder particles, and evolve the required microstructure. In developing a heat treatment for the A-W material the approach taken was to identify the optimum nucleation temperature (ONT), as this is the temperature at which a hold in the heat treatment is desirable in order to allow the maximum number of nuclei to form, such that high levels of crystallisation occur. A further temperature hold after nucleation is required to promote crystal growth. The temperature for this crystallization treatment was selected on the basis of DTA analyses to favour the crystal

propagation of apatite and wollastonite simultaneously [16]. This process resulted in the post-processing regime shown in Figure 1.

Material	Laser Power (W)	Beam Diameter at Bed (mm)	Scan Speed (mm/s)	Scan Overlap (%)	Depth of Spread Layers (mm)
A-M	12	1.1	150	50	0.25
A-W	5	0.55	150	50	0.125

Table 1 – Processing Conditions

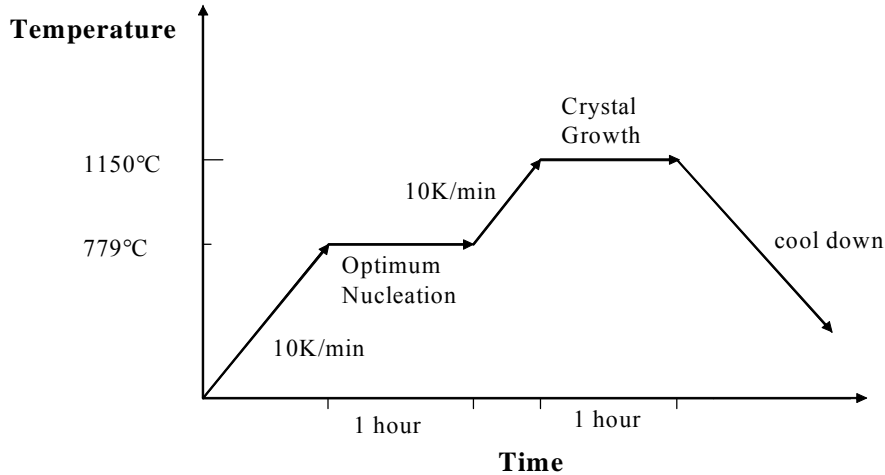


Figure 1 – A-W Heat Treatment Regime

A similar approach was initially taken to the development of a heat treatment regime for the A-M material, but proved unable to create components with any significant strength. For the A-M material it appears that the nucleation process removes too much of the glassy phase of the material, and, as it is the glassy phase which provides the material for liquid phase sintering, this produced components with very low strengths. The solution to this problem was to use a heat treatment which involved putting the green parts directly into a furnace at 1200°C, holding at this temperature for an hour and then cooling at the natural rate of the furnace. When the material is placed directly into a very hot furnace there appears to be enough time for liquid phase sintering to occur before crystallisation, hence stronger parts can be produced.

After sintering the A-M and A-W components were 50-60% dense, and had open porous structures favourable for bone ingrowth and vascularisation. Figure 2 shows a comparison the of microstructures before and after heat treatment of A-W. The pores are relatively small, but macroporosity can clearly be created at the SLS stage. A-M showed a very similar response. For some components further post-processing was undertaken in order to infiltrate the components with phosphate glass. The aim in doing this was to increase the strength of the components, and to increase the bioactivity through offering a combination of two bioactive phases. The infiltration was carried out by placing phosphate powder on top of a sintered part within a vacuum furnace, then heating at 10°C/min to 1200°C, holding at that temperature for an hour, and cooling at the natural rate of the furnace. The infiltration process produced parts in which the porosity had been almost completely eliminated.

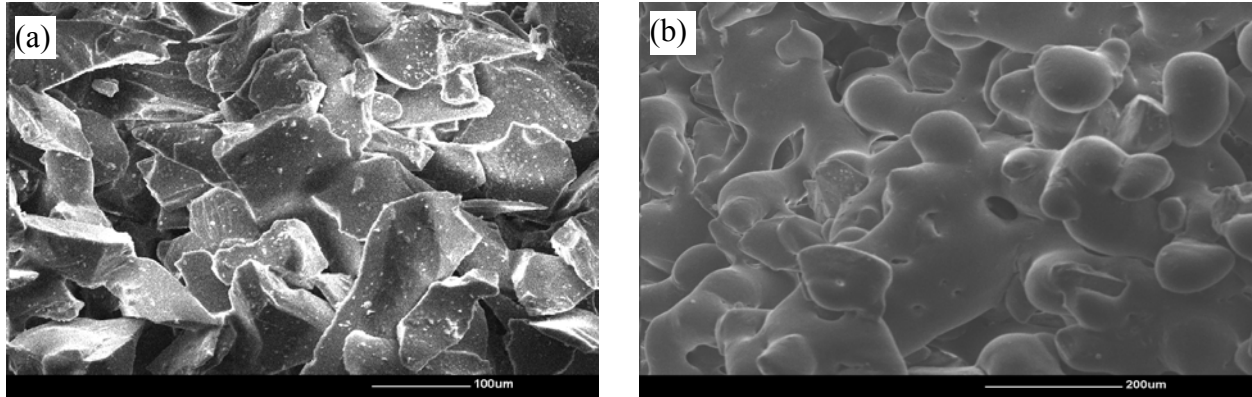


Figure 2 – (a) A-W Green Part, (b) A-W Brown Part

3. Mechanical Properties

The mechanical properties of the components have been investigated using three point bend tests. Specimens nominally 25mm x 4mm x 3mm or 20mm x 3mm x 3mm were produced according to the processing conditions described above, with the span in the bend test either 20mm or 15mm depending on the original length of the sample. All the tests were carried out at room temperature and the speed of the moving support was 2mm/s. The peak force recorded was used to calculate the flexural strength (σ) from [17];-

$$\sigma = \frac{3}{2} \frac{Pl}{ab^2} \quad (1)$$

where P is the loading force, l is the span of two parallel roller supports, a is the width of sample, and b is the thickness of sample.

Figure 3 shows a summary of the measured flexural strengths of samples produced using the materials and processing conditions outlined above, together with the commonly quoted strengths of cancellous and cortical bone [18]. The results show from a baseline figure of 7MPa for A-M that mixing the 45-90 μ m A-M with a proportion of finer powder, or infiltrating with a phosphate glass approximately doubles the strength, to the stage where it is in line with that of cancellous bone. The use of mixed powder size ranges still leaves significant porosity (~40%), and so there is scope to combine these approaches to gain a further improvement in strength. The A-W material is stronger than the A-M material even before any strategies to increase its strength have been implemented, and current work is seeking to employ similar methods to those used with the A-M material to drive the A-W material strength up towards that of cortical bone.

4. Biological Responses

4.1 *In Vitro* – Simulated Body Fluid

The first in vitro approach used relies upon the observation that a prerequisite for an artificial material to bond to bone is the formation of a bone-like apatite layer on its surface when implanted into a bony defect. This same type of apatite layer can be observed on the surfaces of bioactive glasses and glass-ceramics when they are exposed to a simulated body fluid (SBF) [19], and SBF testing is a method of assessing how well bone replacements would be expected to bond

to bone upon implantation. Figure 4 shows the results of an SBF study on samples of A-W produced by indirect SLS, showing that apatite forms on this material very quickly, and that after 14 days a layer which completely covers the A-W material has formed (shown at the top of Figure 4(d), with the A-W at the bottom). These results are extremely positive. As bone growth occurs quickly the rapid formation of the apatite layer means that natural bone *in vivo* would have material which it could bond directly to within a short time of implantation, which would promote bonding as against fibrous encapsulation [15]. This would offer very rapid and natural fixation of an implant, allowing patient mobility to be restored as early as possible after surgery.

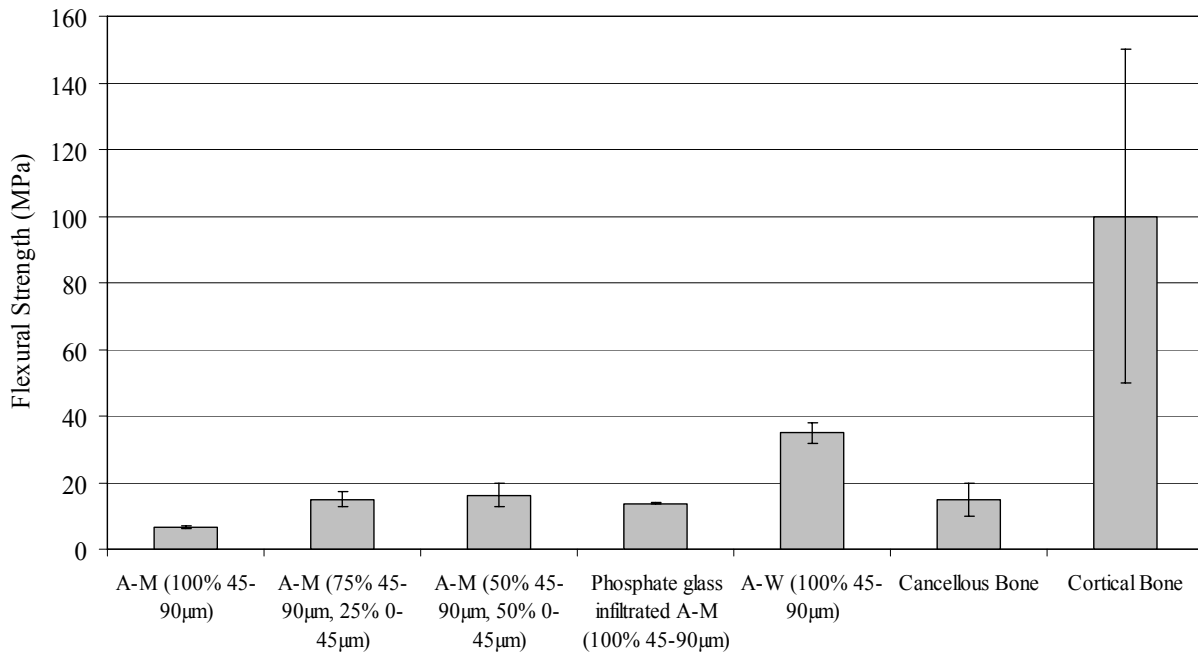


Figure 3 – Summary of Flexural Strength Test Results.
Error bars indicate full range of strengths measured or reported.

4.2 *In Vitro* – Stem Cell Seeding

This set of tests is the first of a series aimed at understanding how well A-W produced using indirect SLS will act as a tissue engineering scaffold. Laser sintered A-W samples with dimensions approximately 3mm x 3mm x 2mm seeded with human mesenchymal stem cells (MSCs). MSCs were extracted from the marrow of femoral heads obtained from routine hip replacement surgery following informed consent. MSCs are multipotent cells that can differentiate into bone forming cells (osteoblasts), as well as cartilage and adipose tissues and are attractive candidate cells for orthopaedic cell-based therapies. MSCs were statically seeded onto A-W scaffolds to assess their ability to attach to the scaffolds surface. To determine the optimal cell seeding density MSCs were seeded at different densities of 1×10^5 , 5×10^5 and 1×10^6 cells per scaffold. The scaffolds were cultured for six hours then analysed for cell attachment by scanning electron microscopy and confocal microscopy as shown in Figure 5. For confocal analysis the MSCs were labelled with a fluorescent dye (Cell Tracker Green) prior to seeding. MSCs successfully attached to and spread on the A-W scaffolds after six hours achieving an even coverage of cells over the seeded surface.

4.3 In Vivo Test Results

For bone replacement materials which have shown promising *in vitro* behaviour the next stage in evaluation is an *in vivo* evaluation. Cylindrical samples of A-M glass ceramic, 4mm in diameter and 10mm in length were produced by indirect SLS. The materials were implanted into the metaphysis of the tibia of six mature male rabbits using strict aseptic surgical techniques, along with samples of commercially available A-W (Cerabone®). The interface between the implanted materials and the surrounding bone four weeks after implantation can be seen in the SEM micrographs shown in Figure 6, where the bone is on the left hand side of the images with the implants on the right hand side. The images show that the bone has grown into the porous implant structure, and that the bone appears to grow right up to the surface of the implanted material. These results confirm the promise shown by the implant structures *in vitro* and further confirm the excellent bioactive behaviour shown by these materials: to all intents and purposes the materials behave *in vitro* and *in vivo* as ideal bone implant materials, able to rapidly bond to bone and showing the same chemical reactions as one would expect from the apatite phase of natural bone.

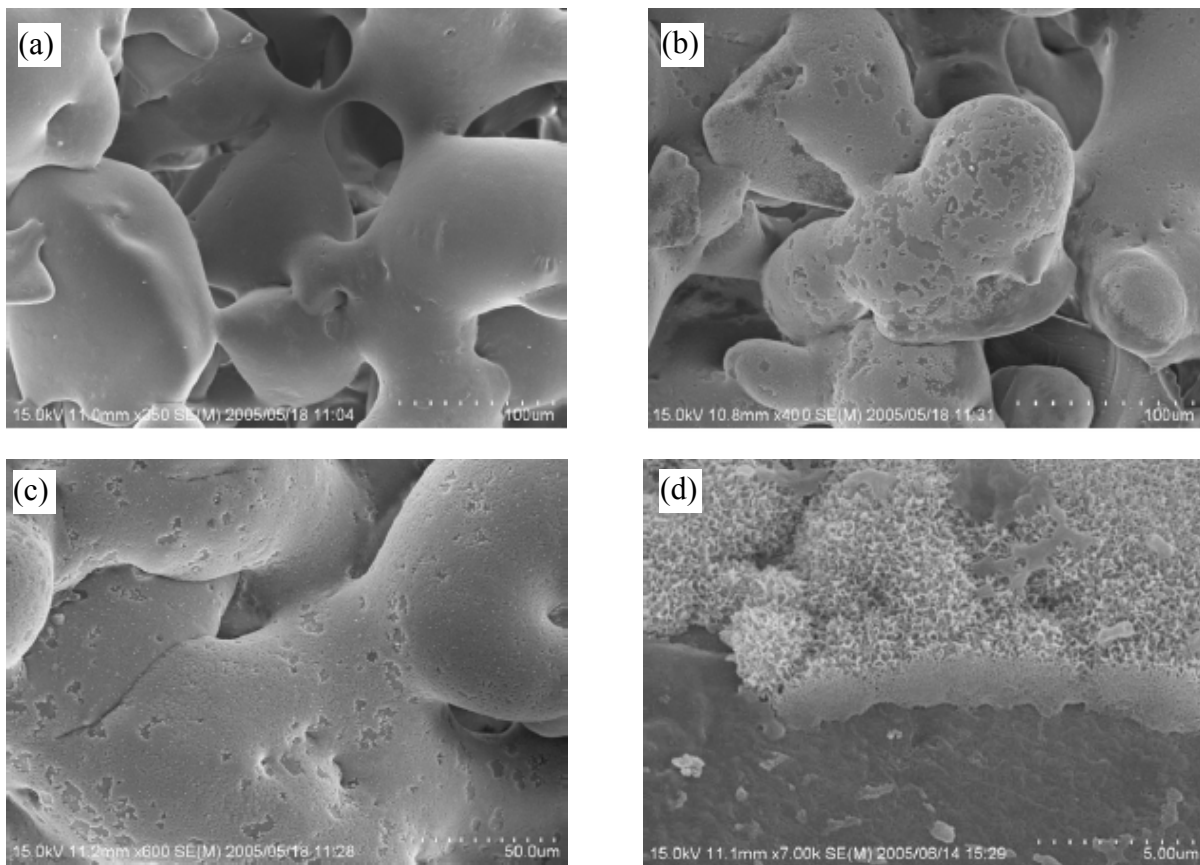


Figure 4 – A-W (a) before SBF testing, (b) and (c) after 1 day immersed in SBF, and (d) after 14 days immersed in SBF

5. Conclusions

- For the A-M material it is clear that the *in vivo* bioactive behaviour is very promising. The strength of this material as processed by indirect SLS is comparable to that of cancellous

bone, indicating that, at this stage, it would be suitable for non-load bearing applications within the body.

- For the A-W material we are at an earlier stage in development. However, A-W processed conventionally is known to exhibit excellent bioactivity, reinforced by Figure 6(b), and the SBF and initial stem cell seeding trials show excellent bioactive potential for A-W produced by indirect SLS. At no point in our studies has the processing route changed the bioactive response of either of the materials examined. In addition A-W produced by indirect SLS also shows excellent mechanical properties, and we are confident that further processing trials will allow us to generate mechanical properties in line with those exhibited by cortical bone.

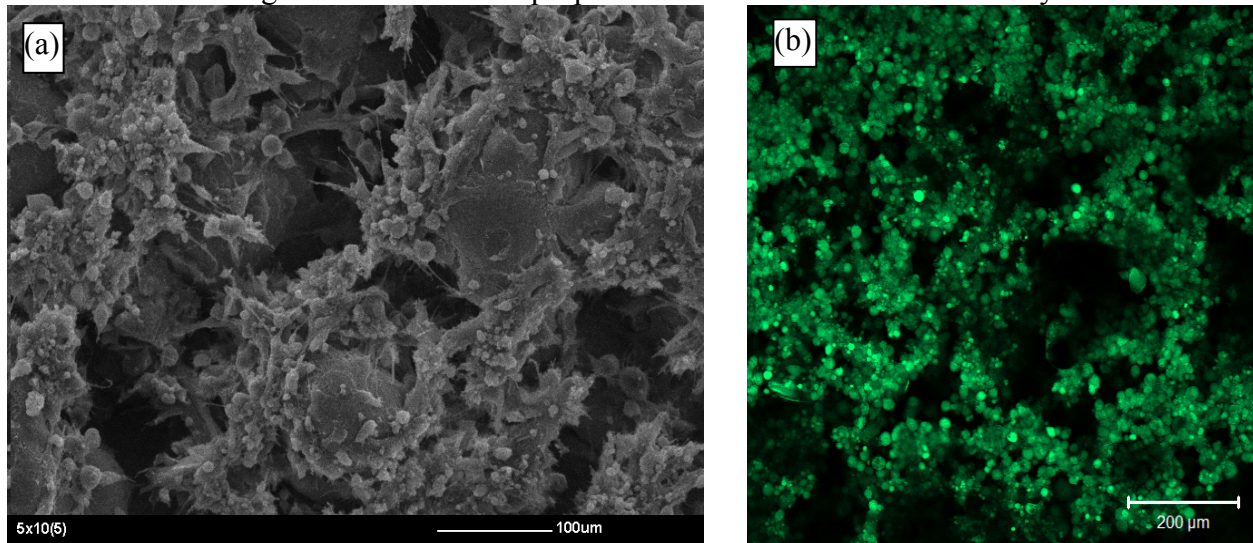


Figure 5 – (a) SEM image of an A-W scaffold 6 hours after seeding with 5×10^5 MSCs, (b) Confocal microscope image of an A-W scaffold 6 hours after seeding with 5×10^5 MSCs. MSCs are fluorescently labelled with Cell Tracker Green. Depth into scaffold is $46 \mu\text{m}$.

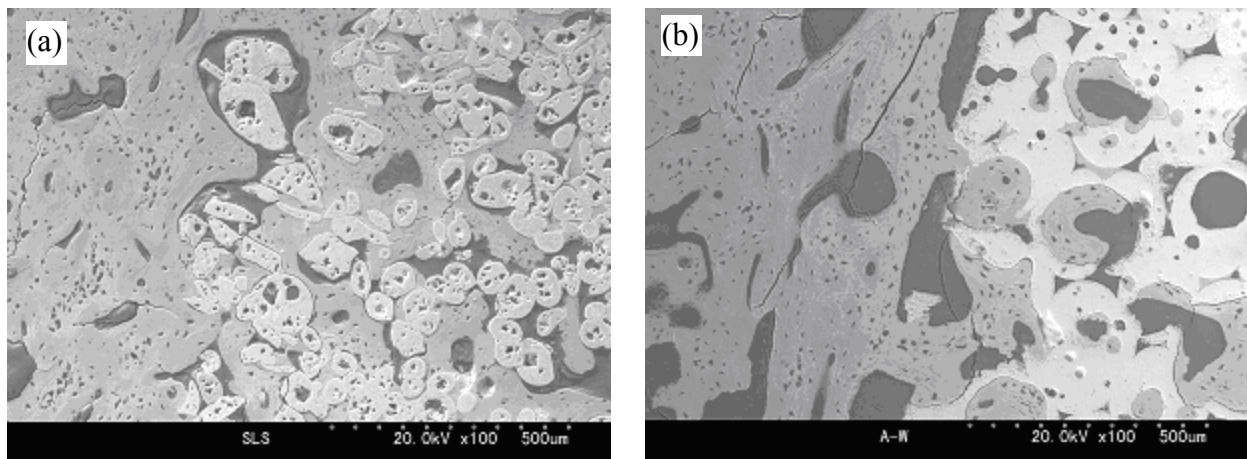


Figure 6 – (a) SEM of implanted A-M material produced by indirect SLS, (b) SEM of implanted A-W material.

References

1. <http://www.therics.com>, 10th May 2005, 09:48 GMT.
2. Gauthier, O., Bouler J.M., Aguado, E., Pilet, P., Daculsi G., 1998, *Macroporous biphasic calcium phosphate ceramics: influence of macropore diameter and macroporosity percentage on bone ingrowth*, *Biomaterials* Vol. 19, pp 133-139.
3. Zein, I., Hutmacher, D.W., Tan, K.C., Teoh, S.H., 2002, *Fused deposition modelling of novel scaffold architectures for tissue engineering applications*, *Biomaterials*, Vol. 23, pp 1169-1185.
4. Ciardelli, C., Chiono, V., Cristallini, C., Barbani, N., Ahluwalia, A., Vozzi, G., Prevet, A., Tantussi, G., Giusti, P., 2004, *Innovative tissue engineering structures through advanced manufacturing technologies*, *Journal of Materials Science: Materials in Medicine*, Vol. 15, pp 305-310.
5. Taboas, J.M., Maddox, R.D., Krebsbach, P.H., Holister, S.J., 2003, *Indirect solid freeform fabrication of local and global porous, biomimetic and composite 3D polymer-ceramic scaffolds*, *Biomaterials*, Vol. 24, pp 181-194.
6. Cooke, M.N., Fisher, J.P., Dean, D., Rimnac, C., Mikos, A.G., 2002, *Use of stereolithography to manufacture critical sized 3D biodegradable scaffolds for bone ingrowth*, *Journal of Biomedical Materials Research Part B: Applied Biomaterials*, Vol. 64B, pp 65-69.
7. Sherwood, J.K., Riley, S.L., Palazzolo, R., Brown, S.C., Monkhouse, D.C., Coates, M., Griffith, L.G., Landeen, L.K., Ratcliffe, A., 2002, *A three-dimensional osteochondral composite scaffold for articular cartilage repair*, *Biomaterials*, Vol. 23, pp 4739-4751.
8. Suchanek, W., Yoshimura, M., 1997, *Processing and properties of hydroxyapatite-based biomaterials for use as hard tissue replacement implants*, *Journal of Materials Research*, Vol. 13, pp 94-117.
9. Sachlos, E., Czernuszka, J.T., 2003, *Making tissue engineering scaffolds work. Review on the application of solid freeform fabrication technology to the production of tissue engineering scaffolds*, *European Cells and Materials*, Vol. 5, pp 29-40.
10. Landers, R., Hubner, U., Schmelzeisen, R., Mulhaupt, R., 2002, *Rapid prototyping of scaffolds derived from thermoreversible hydrogels and tailored for applications in tissue engineering*, *Biomaterials*, Vol. 23, pp 4437-4447.
11. Chu, T.M., Orton, D.G., Halloran, J.W., Hollister, S.J., Feinberg, S.E., 2002, *Mechanical and in vivo performance of hydroxyapatite implants containing controlled internal architecture*, *Biomaterials*, Vol. 23 pp1283-1293.
12. Vail, N.K., Swain, L.D., Fox, W.C., Aufdemorte, T.B., Lee, G., Barlow, J.W., 1999, *Materials for biomedical applications*, *Materials and Design*, Vol. 20, pp123-132.
13. Lorrison, J.C., Dalgarno, K.W., Wood, D.J., 2005, *Processing of an apatite-mullite glass-ceramic and an hydroxyapatite/phosphate glass composite by selective laser sintering*, *Journal of Materials Science: Materials in Medicine*, Vol. 16, pp 775-781.
14. Goodridge, R.D., Lorrison, J.C., Dalgarno, K.W., Wood, D.J., 2004, *A comparison of direct and indirect selective laser sintering of porous apatite-mullite glass ceramics*, *Glass Technology*, Vol. 45, pp 94-96.
15. Goodridge, R.D., 2004, *Indirect selective laser sintering of an apatite-mullite glass-ceramic*, Ph.D. Thesis, University of Leeds, UK.

16. Xiao, K., Dalgarno, K.W., Wood, D.J., 2005, *Selective laser sintering of apatite-wollastonite glass ceramics*, presented at the 6th National Conference of Rapid Design, Prototyping and Manufacturing, held at Buckinghamshire Chilterns University College, High Wycombe, UK, 10th June 2005.
17. ISO 14125, 1998, *Fibre-reinforced plastic composites - determination of flexural properties*.
18. Hench, L., Wilson, J., 1993, *An introduction to bioceramics*, World Scientific, Singapore.
19. Kokubo, T., Kushitani, H., Ohtsuki, C., Sakka, S., 1992, *Chemical reaction of bioactive glass and glass-ceramics with a simulated body fluid*, *Journal of Materials Science: Materials in Medicine*, Vol. 3, pp 79-83.